Status of the LHCb experiment

CERN-RRB-2016-107

October 2016

1   Introduction

LHCb continued its successful data taking in Run 2 and has so far accumulated a total of 1.4 fb^{-1} in pp collisions with a global efficiency of around 88%. All sub-detectors were fully functional and acquired high-quality data. Improvements have been implemented to the experiment's revolutionary real-time alignment and calibration procedure. The status of the sub-detectors and of the operation of the experiment are summarised in Sects. 2 and 3, respectively.

The LHCb collaboration has continued to release physics results of high scientific interest. A total of 334 papers have now been submitted to journals and several preliminary results have been shown at conferences. Recent highlights include heavy flavour [1, 2] and gauge boson [3] production, observation of new exotic states [4, 5], rare decays in the strange [6] and beauty [7] sectors, radiative decays [8], and CP violation in charm [9–11] and beauty [12–14]. Selected physics results are presented in Sect. 4.

Financial issues and collaboration's matters are reviewed in Sects. 5 and 6, respectively.

Finally, significant efforts have been invested into preparations for the LHCb Upgrade, scheduled to be installed in Long Shutdown 2. This work is described in a separate document [15].

2   Detector sub-systems

Over the last six months the operation of the LHCb detector has been very smooth and the data taking extremely efficient. Only very few minor issues required an access to the experimental cavern for detector inspection or exchange of electronic components. A construction of a partial magnet mock-up was completed; this model is used for the training of specialists to prepare them for an efficient exchange of the magnet cooling pipes in case a leak develops and a fast intervention is required. Early this year the new LHCb control room was commissioned and was

soon fully operational. The focus is now on the preparation for the extended year-end-technical-stop (EYETS) during which the personnel lift and the main equipment for the two 40 t cranes in the cavern are scheduled to be exchanged. This intervention will occupy almost the full duration of the EYETS, so that detector-related activities occurring in parallel will have to be planned carefully.

2.1 Vertex Locator (VELO)

The VELO has been taking high-quality data very efficiently throughout physics running in 2016.

Several maintenance activities were performed. In 2015 a large build-up of ice from condensation was observed in the CO_2 cooling plant. Melting ice poses the risk of overflowing the reservoir at the bottom of the cooling plant, which would trigger a DSS interlock that cuts the chilled water supply to LHCb. To mitigate this risk, the cooling plant was sealed and a dry air circulating system installed, after first removing the ice and replacing the pipe insulations. A faulty ground connection that caused a malfunction in the cooling PLC was repaired. One TELL1 readout board and one low-voltage power-supply module were replaced. These interventions did not cause any data loss.

Due to the extremely high availability of the LHC, the VELO received a higher radiation dose than anticipated. Thus a careful monitoring of radiation-damage effects is more important than ever. Several CCE (charge collection efficiency) scans were recorded to determine the effective depletion voltage of the VELO sensors. The analysis results suggest that the VELO sensors with the highest radiation damage are slightly under-depleted in their innermost regions. There are plans, therefore, to raise the bias voltage for these sensors from 250 V to 300 V.

It has been intended to deploy the automated recording of IV scans after each fill. However, this plan has had to be revised because of the increased efficiency of the LHC and very short time between fills. The scans are now performed on request of the VELO on-call expert in coordination with the LHCb shift leader. The maximum voltage for the IV scans has been raised from 250 V to 300 V, and no HV channel trips have been observed, in contrast to tests performed earlier this year. This gives confidence that the HV system will be stable when the bias voltages are raised. The results of a scan as displayed by the VELO expert monitoring system are shown in Fig. 1.

2.2 Silicon Tracker (ST)

The Silicon Tracker consists of two sub-detectors, the Tracker Turicensis (TT) and the Inner Tracker (IT). Both detectors are operated by the central LHCb shift crew with support from an on-call piquet and a small, dedicated team of experts. There have been no major problems during 2016 and the fraction of working channels is currently 99.55% and 98.97% in TT and IT, respectively.
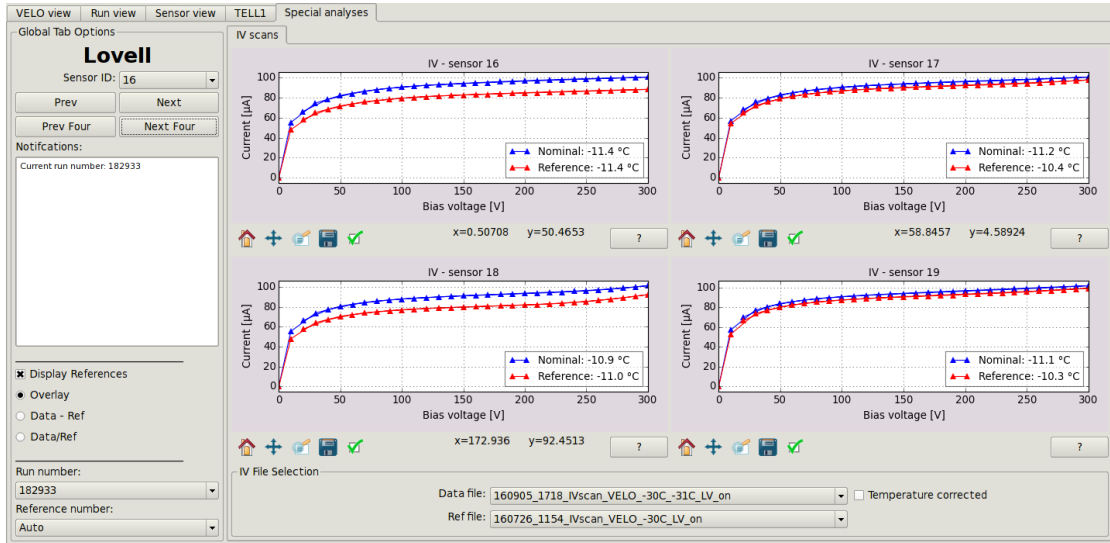
Figure 1: The IV scan results for four VELO sensors as displayed by the VELO expert monitoring system. New results are shown in blue (higher curves) and reference measurements in red (lower curves). The slightly higher currents due to increased radiation damage are expected.

The fraction of working channels in the IT is around 0.3% lower with respect to the number reported in the previous RRB document [16] as one full module stopped working shortly after the detector stations were closed. This module was disabled throughout Run 1 and was only recovered during LS1 when the detectors were opened and it was possible to access the read-out electronics. The module worked without problems during 2015 and attempts will be made to resurrect it during the EYETS.

One TT read-out sector has slowly developed a problem where every fourth channel has an anomalously low level of noise. This behaviour was observed in ∼ 10 modules shortly after installation. The bond wires between the innermost bond row on the read-out chip and the pitch adaptor were found to break over time. New hybrids were produced with an increased distance between the pitch adaptor and the chip, and nine modules were removed from the detector and repaired during the 2010 shutdown. Spare hybrids are still available and this problematic module will be removed and repaired during the EYETS.

The problem with multiple trips of one HV channel in the TT that was reported previously [16] is now under control. However, three CAEN HV boards developed faults on single channels and had to be replaced. The broken boards have been sent to the manufacturer for repairs.

The detector ageing is monitored via measurements of the leakage current and the depletion voltage of the sensors. As for the VELO, the depletion voltage is determined from dedicated CCE scans that are taken at regular intervals during the run while the leakage currents are continuously monitored. The measurements

are compared to predictions from simulation and the radiation damage observed is found to be consistent with expectations.

2.3 Outer Tracker

The Outer Tracker (OT) ran smoothly throughout the luminosity harvest in the spring and summer of 2016. Noisy channels and faulty hardware remain at a negligible level. In August one faulty HV board had to be replaced (which affected 256 straws out of a total of 53760 during one fill), and in September one faulty frontend board was also replaced (affecting 64 straws).

Two operational aspects have required special attention in the last few months of data taking:

- An increasing number of occurences of desynchronising electronics has been observed. To address this concern, an attempt is being made to improve the trigger and clock signals.

- Since LHCb operates at twice the design instantaneous luminosity, the total data volume from the OT approaches the maximum bandwidth that the data acquisition system can digest. Interesting options are being considered to reduce the number of OT spillover hits, which may also benefit the track reconstruction.

The OT time and position alignment is becoming increasingly more sophisticated. The RASNIK hardware alignment system, which was used in the past as an "alarm" system to detect large displacements, is now being deployed as an aid to the software alignment by providing information on small movements. The time measurements in the OT have reached an impressive precision in Run 2 thanks to the online calibration of a global time offset, and thanks to a finer granularity of the time constants. The single hit time resolution has reached a value as low as 2.4 ns, which results in a precision of the time-stamp per track below 600 ps. Studies are being performed on how this information can be used for particle identification in physics analyses.

2.4 RICH system

The RICH system has been operating well throughout the 2016 run. The usual calibration procedures were followed, with magnetic distortion calibration system (MDCS) scans, ion feedback runs and timing scans, all showing that the photon detectors are in good health. A very small number of the frontend electronic components have started to show increased sensitivity to upsets. This is under investigation using the latest technical stop to modify settings and change components. It is hoped that these investigations will lead to an improved stability for the whole RICH system.
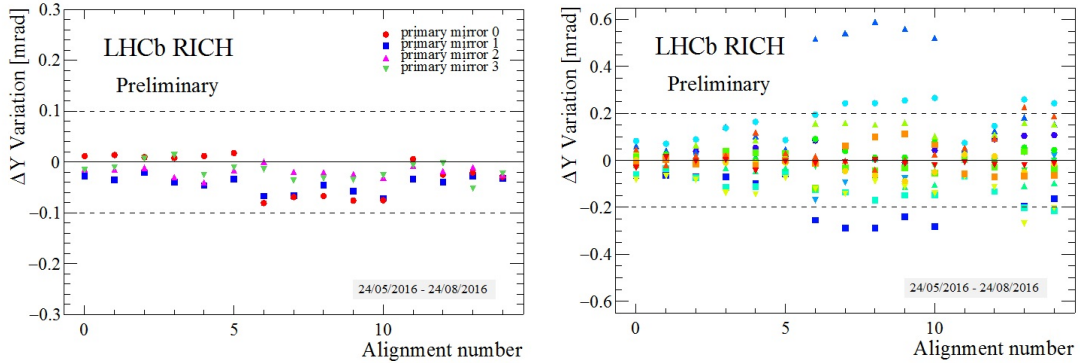
Figure 2: Variation of the RICH1 mirror segment rotation in the local y coordinate versus time (alignment number). The primary mirrors (left plot) show very good stability. A small number of secondary mirrors (right plot) show a different orientation between alignments with magnetic field up (alignment 6-10) and down.

The LHC technical stops were reorganised early in the year and the planned purification of the RICH1 gas was moved from May to the MD period in July. The purification worked well, reducing the amount of nitrogen from about 2% to below 0.3%. However, the restart of the gas system caused a significant argon contamination (up to 40%) that was picked up by the RICH pressure sensors. The gas group was promptly notified and restarted the purification cycle resulting in a clean gas in time for physics data. The adopted strategy of minimising risk by performing operations such as gas purification outside data taking periods worked very well.

The automatic run-by-run calibrations have been working seamlessly since the start of 2015. The start of 2016 also saw the mirror alignment running automatically at every fill. With a lot more data available for the mirror alignment it is possible to understand much better any mirror movements (see Fig. 2). The system appears very stable. However, there are hints that changing the magnet polarity has some effect on the RICH detectors. The effect is too small to affect the particle identification performance, but it is visible in the Cherenkov angle resolution.

2.5 Calorimeters (SPD, PS, ECAL and HCAL)

The calorimeters have been running smoothly since the beginning of the run. There is currently a small number of dead and noisy detector elements: 64 dead cells, corresponding to one multi-anode PMT, and two noisy cells out of 6016 in the PS and two dead and one noisy cells out of 6016 in the ECAL, as can be seen in Fig.3. The dead cells can only be fixed during the EYETS because this requires opening the detectors.

The initial detector calibration was based on the following procedure:
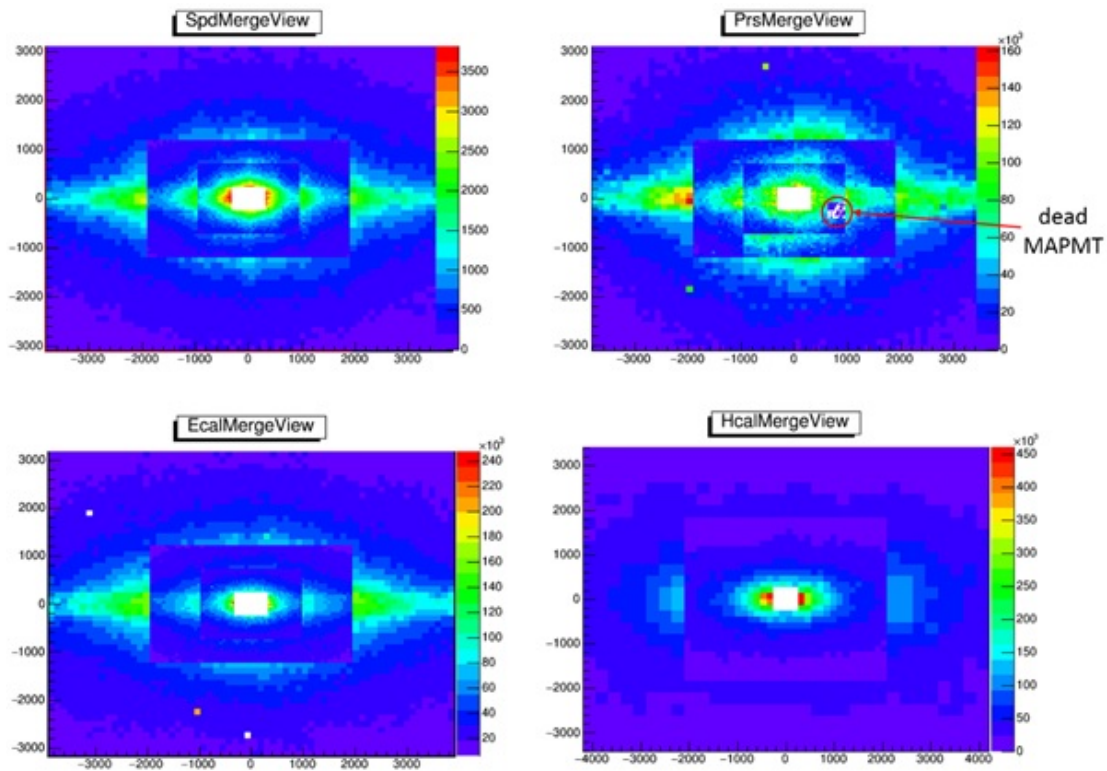
Figure 3: Merged view of CALO detectors based on 51k events.

- HV settings for the HCAL PMTs were obtained from a calibration run with a ^{137}Cs source performed right before the LHC start-up;

- time alignment constants for all calorimeters were updated using data from first collisions;

- for the ECAL calibration, the period of the LHC intensity ramp was used to collect a large sample of $\pi^0 \rightarrow \gamma\gamma$ events; the data were processed using the standard π^0 calibration and the HV settings for the ECAL PMTs obtained from these data were subsequently applied.

During data taking, an automatic HV correction based on the LED monitoring system was used for both ECAL and HCAL. This system efficiently stabilises the PMT gains by adjusting the HV settings after each fill. In addition, for the HCAL, calibration runs with the ^{137}Cs source were performed during the June and September technical stops. Figure 4 shows the variation of the average LED signal amplitude for the central parts of ECAL and HCAL during the 2016 data taking. The dip in the ECAL trend plot in the period 12-19 July corresponds to the failure of an optical mezzanine of a Calorimeter Readout Card (CROC), which resulted in 64 non-operational cells. This problem was fixed during an access around a week later.
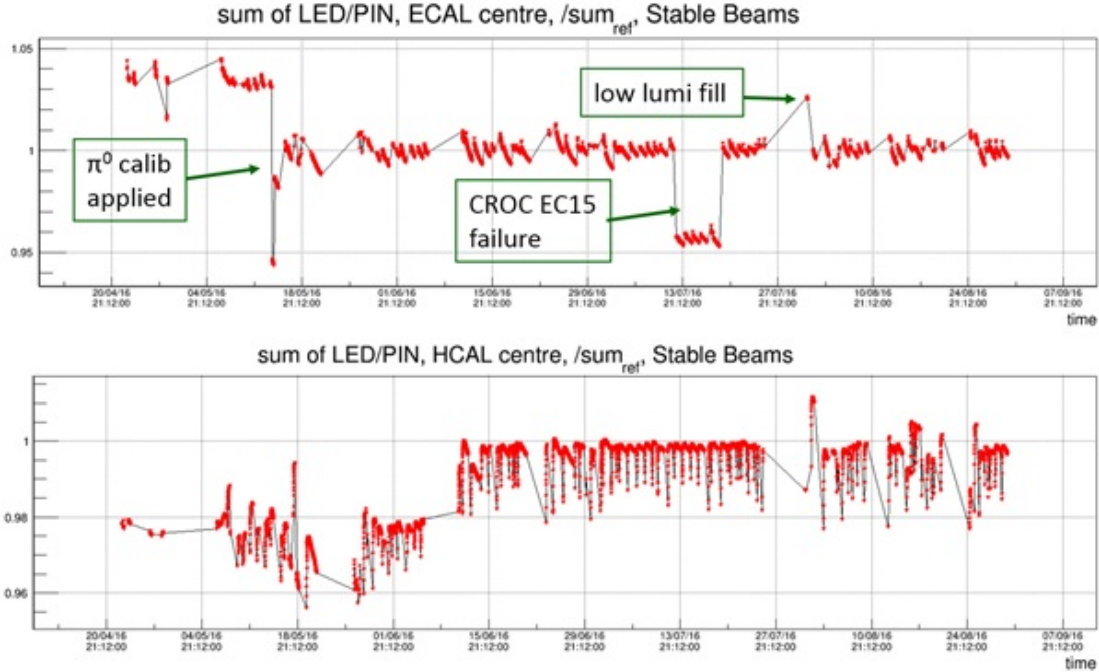
Figure 4: Trend plots of the average LED signal amplitude for the central parts of ECAL (top) and HCAL (bottom) during the 2016 data taking.

2.6 Muon system

After the winter shutdown and the recommissioning phase that took place in the first months of 2016, the muon system resumed successful data taking for the second year of Run 2. The muon system timing was checked and finely adjusted with first collisions. The spatial alignment was also checked with the same data, allowing an improvement to the position of the stations before the increase in LHC luminosity.

Almost 100% of the channels are in operation, with only half a chamber not responding in M1 (from a total of 1380 chambers) and a few non-operating channels in M4R2 and M5R4. During the weeks when the LHC luminosity was rapidly raised a larger than usual number of MWPCs suffered HV trips, which were recovered with the usual training procedures. The situation is now much improved and there is currently a normal MWPC HV trip rate of about one per week, with less than 0.2% of the MWPC gaps kept under HV training.

On the ECS side the improvements performed during the winter shutdown have shown to be very effective and no more Service Board system crashes were reported, although some limited and occasional problems with few ELMBs remain. These issues have no impact on the data taking and will be addressed during the EYETS. Several improvements were implemented in the HV and gas monitoring system. The water and oxygen content are now continuously monitored also for the GEMs and alarms are generated under abnormal conditions. A GEM HV
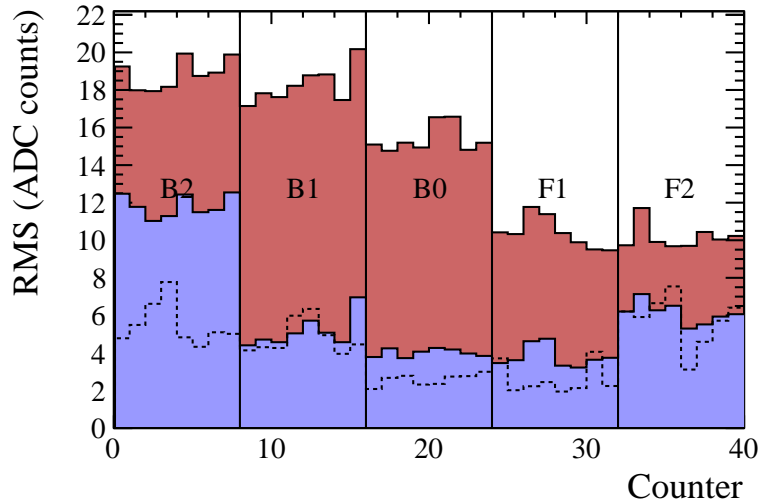
Figure 5: Demonstration of the improved HeRSCheL calibration procedure. The plot compares the uncorrected signal in end-of-fill data taken during 2015 (red filled histograms), that after calibration (blue filled histogram) and the raw signal RMS with the new adapter board in 2016 (dashed histogram). Each station houses four PMTs, read out via the dual-channel VFE board, and there are therefore eight channels to consider for each station. The relatively large noise contribution to the signal from the B2 station was the result of imperfect grounding; this was resolved before 2016 data-taking began.

software protection system was implemented, to be able to detect over-currents or discharges, and then to take appropriate action. The muon chambers have been operating in a very stable manner for many months, with station efficiencies exceeding 98%.

2.7   Forward shower counters (HeRSCheL)

The HeRSCheL detectors, first installed in 2015, collected data for the vast majority of the 2016 LHC run. Further integration was achieved through the addition of information from HeRSCheL in the lowest level of the LHCb software trigger, significantly reducing the bandwidth required for those triggers associated with the Central Exclusive Production physics programme.

Building on the preliminary calibration of 2015 HeRSCheL data, the calibration method was improved and the procedure to implement the common mode subtraction globally, for all users, was defined. The addition of the new analogue board as an adapter between the PMTs and the readout electronics brought a large reduction in noise, reducing the need for offline calibration. The new board results in a noise level in 2016 that is comparable to that achieved after offline calibration in 2015, as shown in Fig. 5. New procedures have been implemented to allow a daily, automatic monitoring of the ageing of the scintillators in response to their

irradiation, and progress is ongoing to automate the preparation of new hardware recipes to adjust the HV and timing settings of the detector to compensate for the ageing. Plans are underway to prepare for replacement of some or all of the scintillators during the EYETS.

A major priority for the EYETS is the inclusion of the HeRSCheL response in the L0 hardware trigger. Following the development of the firmware for the trigger FPGA earlier in the year, work is now focusing on the completion of the trigger chain, and adjustment of the L0 decision unit to include this new input.

2.8 Online system

The most challenging operational issue associated with the High Level Trigger (HLT) farm was the frequent deaths of the locally installed disks on the Dell nodes. Recovering the data from the broken devices, and then replacing the disks, placed an extremely severe burden on the system administration and online teams. To eliminate this problem, the $\sim$500 Dell nodes are being replaced by 300 nodes of the latest generation, resulting in a small, overall increase in available CPU power and a net increase in disk buffer space of $\sim$1.6 PBytes. No other major changes were implemented and the system in general runs very stably. Minor improvements to make the operation of the experiment easier for the shift crew are being constantly applied.

3 Operations

At the time of writing LHCb has so far collected a total integrated luminosity of ~ 1.4 fb^{-1} during the 2016 run, with a global efficiency of around 88%. Figure 6 summarises the delivered and recorded luminosity and the LHCb data collection efficiency.

After gradually increasing the number of bunches in the machine, the instantaneous luminosity at LHCb plateaued at a mean value of 3.7×10^{32}cm^{-2}s^{-1}, with 2036 bunches colliding. The luminosity was levelled throughout to deliver an average number of visible pp interactions per bunch crossing (μ) of 1.1.

The first week of data taken at the end of April was used for detector commissioning. After a first period with limited availability of the LHC machine, an intense period followed in which the beam availability reached 80% for an entire week. Globally, up to now the beam availability has been more than 50%, also including machine development periods. Given that the LHCb trigger had been optimized for an availability of 40%, a trigger reoptimisation was required to maintain a safe filling rate of the online farm disk buffer. Details are provided in Sect. 3.1.

The Turbo stream provides a framework in which physics analysis can be performed directly using the trigger-reconstructed candidates, which implies a much smaller event size. This is illustrated in Sect. 3.2 together with new developments
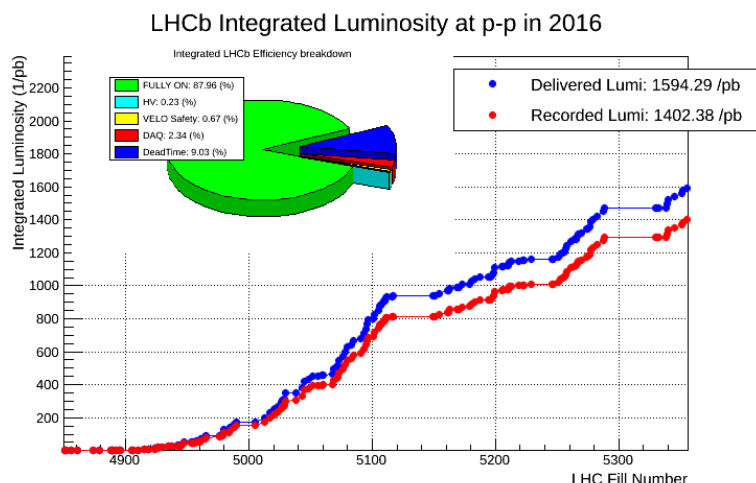
Figure 6: Delivered and recorded integrated luminosity for 2016 up to 6/10/16, and corresponding LHCb efficiency

on how to cope with the increased data volume.

In Run 2, information from the RICH and CALO detectors is included in the full event reconstruction performed at the second level of the software trigger, HLT2. This additional information, coupled with the novel real-time detector alignment and calibration, allows selections in HLT2 (the second stage of the software trigger) to take advantage of offline-quality PID discriminating variables. These variables are used extensively to increase signal purity, reduce the processing time required to reconstruct high-multiplicity signal decays, and reduce biases on quantities of physical interest, such as decay time. The new results from the alignment and calibration are presented in Sect. 3.3, while more information on the new techniques to produce PID-samples is provided in Sect. 3.4.

3.1 Trigger

Prior to the 2016 run, the online-farm disk buffers were un-mirrored to nearly double their capacity to 10 PB. These disks are used to collect data exiting HLT1, the first stage of the software trigger. This increase in capacity allowed more data to be stored, prior to the deferred execution of HLT2. Under the assumption of a maximum 40% average machine availability in 2016, the HLT1 thresholds had been tuned to an output rate of 150 kHz, for which the disk occupancy was projected to gradually increase throughout the year, with a reasonable safety margin. Adjustments in the trigger settings and software were therefore needed to adjust to the exceptional LHC June conditions, with an availability above 70% for three weeks. Profiting from the HLT flexibility, it was possible to improve significantly the purity of the HLT1 selections, and reduce the rate to 80 kHz, while maintaining a high efficiency. In particular, the RICH reconstruction software was optimised,

producing a gain of several percent in the HLT2 throughput. A further 5-10% improvement, depending on the specific running conditions, was achieved with the exploitation of the NUMA memory management option for multiprocessing applications and from the fine tuning of the multiprocessing parameters.

Approximately 500 pb^{-1} of data were recorded with the tight HLT1 configuration, reaching a disk usage of around 60% just before the first machine development. In July, when the machine efficiency decreased, it was possible to revert to a looser HLT1 configuration tuned to an output rate of around 110 kHz.

3.2 Turbo stream

The Turbo stream provides a framework in which physics analysis can be performed using directly the trigger-reconstructed candidates, which requires a much smaller event size. A new relevant feature, implemented in 2016, is the ability to save the entire trigger-reconstructed event. This improvement has allowed the majority of the LHCb physics analyses to migrate to the online Turbo reconstruction. However, this has also led to an increase of the Turbo output bandwidth by more than a factor of three and to a significant increase of the Turbo dataset size for 2016. To be able to deal with this, the ability to 'park' data has been introduced. Moreover, to facilitate data analysis, the Turbo stream has been split into multiple streams. Further innovations are foreseen for 2017 to again reduce the size of the Turbo-recorded events.

3.3 Calibration and alignment

The real-time alignment tasks were fully commissioned in 2015. The procedure has been running smoothly since the beginning of the 2016 data taking with an automatic update of the alignment constants for VELO and IT, while it is run in monitoring mode for the RICH mirror alignment and the muon alignment. Figure 7 shows the relative variation of the alignment constants determined by the procedure with respect to the used constants for VELO and IT. The VELO alignment is typically updated every ∼five fills, while the IT alignment is updated every week.

Figure 8 shows the relative variation of the alignment constants for the muon chambers and the RICH1 primary mirrors. After the first alignment evaluation with 2016 data, the subsequent variations are small enough (less than 1 mm for the muon chambers and less than 0.1 mrad for the RICH mirrors) not to affect the physics performance, hence no further updates were applied.

The RICH calibration and the OT time calibration run routinely for each run with automatic updates applied when required.

The calorimeter is calibrated on a fill-by-fill basis by an automatic LED calibration. This allows compensation for PMT ageing, resulting in a LED gain stability within a few percent throughout the entire 2016 data taking period. The absolute ECAL calibration is evaluated by studying the π^0 invariant mass distribution on
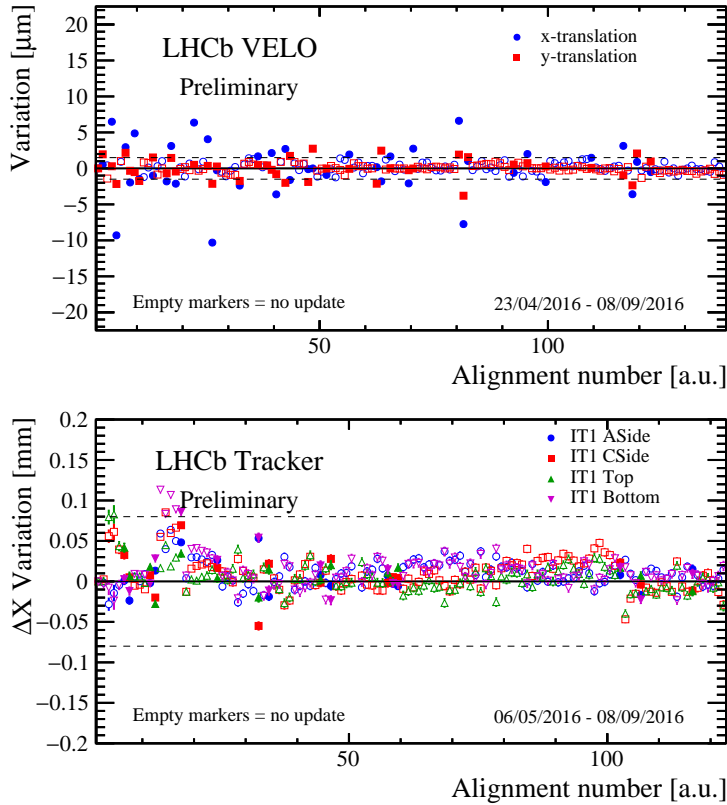
Figure 7: Stability of the VELO (top) and of the IT boxes (bottom) alignment constants during the first part of the 2016 data taking. The dashed lines indicate the minimum variation to consider significant the alignment difference. Each point shows the variation of the alignment parameter with respect to the used constants. The filled markers indicate when an alignment update was needed.

a cell-by-cell basis. The π^0 calibration is currently under a complete review to be able to allow for a full automation of the procedure.

3.4 Particle Identification

Pure data samples of pions, kaons, protons, muons and electrons are selected for calibration, in order to allow efficiencies to be determined in a data-driven manner. The selection of calibration samples is mainly implemented in a set of HLT2 lines grouped in the so-called "TurboCalib" stream. Events in this stream are processed so that online and offline variables are simultaneously available. In this way the same particle decay candidates can be used to provide data driven corrections for both the online and offline event reconstructions.
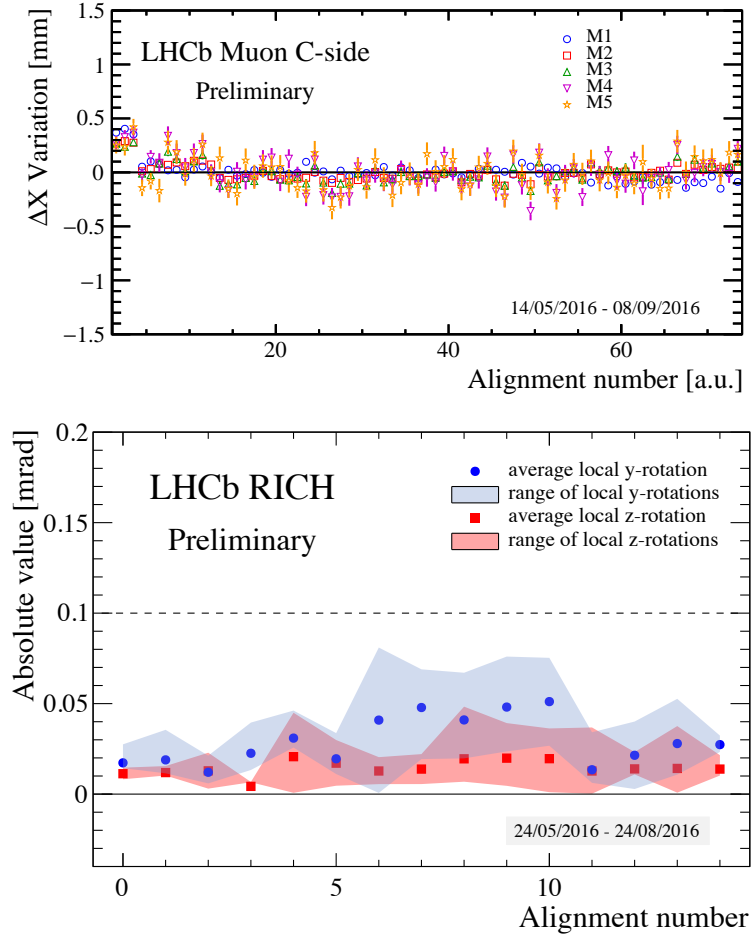
Figure 8: Top: stability of the alignment constant for the $x-$translation of the muon C side chambers, during the first part of 2016 data taking. Each point shows the variation of the alignment parameter with respect to the used constants. Bottom: stability of the RICH primary mirror during the first part of 2016 data taking. Each point shows the average variation for the $y-$rotation (blue points) and the $z-$rotation (red points). The corresponding bands show the range of the variation.

3.5 Data-quality monitoring

The data quality (DQ) in Run 2 consists of two steps: (i) real-time monitoring performed by the data manager at the pit to guarantee that no major failures are affecting data taking; (ii) DQ-checking and flagging of the post-HLT2 data to be used for physics analysis. In Run 1 this second step was performed after offline processing of the data, introducing a delay of the order of days. In Run 2 a so-called "prompt DQ" is designed to flag the data only a few minutes after HLT2 processing. Only in the case of very short runs or poorly understood behaviour will the full offline-DQ be run.

The DQ system was fully commissioned at the restart of Run 2 in 2016 and regular DQ shifts have been organised. The new DQ framework is web-based so that remote shifts are possible. The "prompt DQ" worked successfully from day one, allowing a fast problem detection and solution during restart. Work is ongoing to also migrate the real-time monitoring to the new web-based framework. The same framework is also being used to monitor the quality of simulated data.

3.6 Offline processing

The computing usage in the first half of 2016 [17] and the re-assessed estimates for 2017, incorporating the increased LHC efficiency and requests for 2018 and 2019 [18], are discussed in detail in separate documents.

4 Physics results

Since the last RRB in April 2016, LHCb submitted 22 new publications, for a total of 334 papers at the time of writing. Sixteen further publications are being processed by the Editorial Board and are close to submission. In the following, some results in the sectors of heavy flavour, exotica and gauge boson production, rare and radiative decays, and CP violation are highlighted.

4.1 Heavy flavour, exotica and gauge-boson production

Central exclusive production of J/ψ and $\psi(2S)$ mesons at a centre-of-mass energy of 13 TeV was measured [1]. Owing to the use of new HERSCHEL detector, backgrounds are significantly reduced compared to previous measurements made at lower energies. The cross-section times branching fractions for the decays to dimuons, where both muons are within the pseudorapidity region $2 < \eta < 4.5$, was measured differentially in ten bins of pseudorapidity for the J/ψ meson and in three bins for the $\psi(2S)$. Good agreement was observed with NLO theoretical predictions, as shown in Fig. 9 for the J/ψ cross-section.

A new measurement of the beauty production cross-section at 7 and 13 TeV centre-of-mass energy as a function of the pseudorapidity was performed in the range $2 < \eta < 5$ [2]. The measurement is based on semileptonic decays of b-flavoured hadrons decaying into a ground-state charmed-hadron in association with a muon, and summing the rates. The agreement with theoretical expectation is good at 7 TeV, but differs somewhat at 13 TeV. A disagreement with theoretical expectations is observed between the ratio of the 13 to 7 TeV cross-sections in the low η region.

New exotic states were observed by means of the first full amplitude analysis of $B^+ \to J/\psi\phi K^+$ with $J/\psi \to \mu^+\mu^-$, $\phi \to K^+K^-$ decays, performed with the full Run 1 data sample [4, 5]. The data could not be described by a model that contains only excited kaon states decaying into ϕK^+, and four $J/\psi\phi$ structures
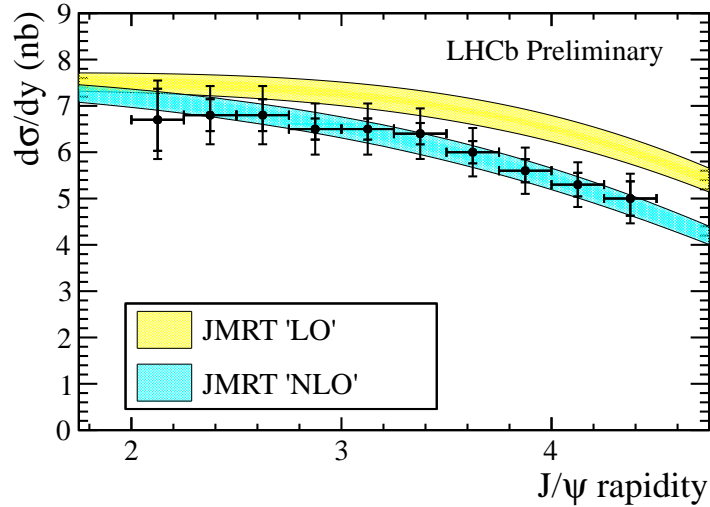
Figure 9: Differential cross-section compared to LO and NLO theory JMRT predictions for J/ψ central exclusive production. The inner error bar represents the statistical uncertainty, and the outer the total uncertainty.

were observed, each with a significance exceeding five standard deviations. The quantum numbers of these structures were determined with a significance of at least four standard deviations.

A measurement of the production cross-section of Z bosons at 13 TeV was performed using di-muon and di-electron final states [3]. The integrated cross-section was measured for leptons with pseudorapidity in the range $2 < \eta < 4.5$, transverse momenta $p_\mathrm{T} > 20$ GeV and di-lepton invariant mass in the range $60 < m(ll) < 120$ GeV. In addition, differential cross-sections were measured as functions of the Z boson rapidity, transverse momentum and the angular variable ϕ_η^*.

4.2   Rare and radiative decays

In the sector of strange physics, a search for the rare decay $\Sigma^+ \to p\mu\mu$ was performed using the full Run 1 data sample [6]. An excess of events was observed with respect to the background expectations with a signal significance of four standard deviations. The main motivation for this search was due to the findings of the HyperCP collaboration, which ten years ago published the results of a similar search where three events were found, with a di-muon mass clustering around 214 MeV. Hence the HyperCP results were hinting at a possible new resonance. In the LHCb data, no significant structure is observed in the di-muon invariant mass distribution.

Moving to beauty, a search for the pure annihilation $B^0 \to K^+ K^-$ decay was performed using Run 1 data [7]. This decay has been searched for during the last 15 years at the B-factories and at the Tevatron without success. It is now observed for the first time by LHCb with a significance of more than five standard
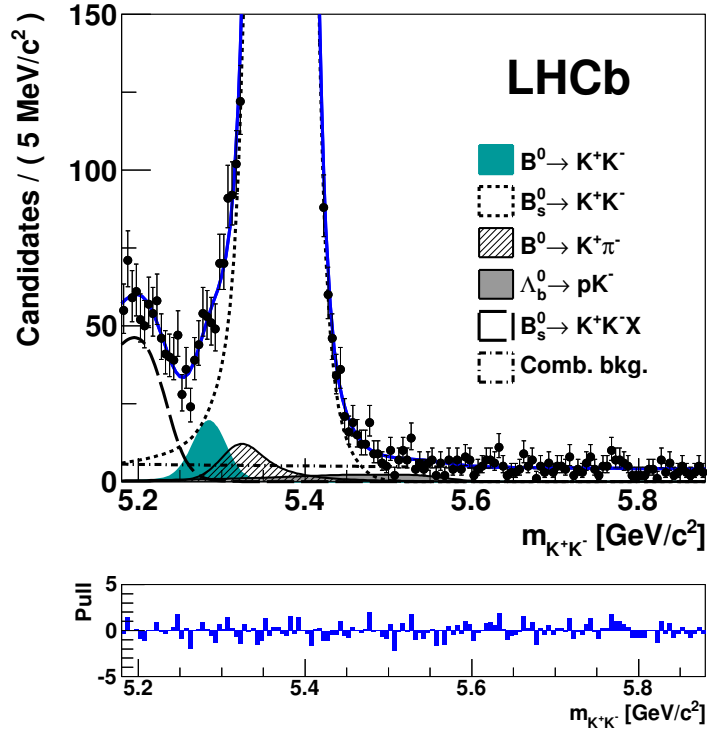
Figure 10: Invariant mass distribution for K^+K^- final states in the search for the rare $B^0 \to K^+K^-$ decay. The result of the fit is superimposed. The various contributions are explained in the legend.

deviations. The K^+K^- invariant mass distribution is shown in Fig. 10. The analysis also results in an improved measurement of the branching fraction for the $B_s^0 \to \pi^+\pi^-$ decay. In particular, the $B^0 \to K^+K^-$ is the rarest B-meson decay to a fully hadronic final state ever observed.

Another noteworthy measurements is that of the polarisation of photons produced in radiative B_s^0 decays. This was studied for the first time using Run 1 data by means of a time-dependent analysis of the $B_s^0 \to \phi\gamma$ decay rate, to determine the ratio of right- over left-handed photon polarisation amplitudes in $b \to s\gamma$ transitions [8]. The result is consistent with the Standard Model prediction within two standard deviations.

4.3 CP violation in charm and beauty

A measurement of the time-integrated CP asymmetry in the Cabibbo-suppressed decay $D^0 \to K^+K^-$ was performed using the full Run 1 data [9]. The flavour of the charm meson at production is determined from the charge of the pion in $D^{*+} \to D^0\pi^+$ and $D^{*-} \to \overline{D}^0\pi^-$ decays. This is the most precise determination of a time-integrated CP asymmetry in the charm sector from a single experiment.
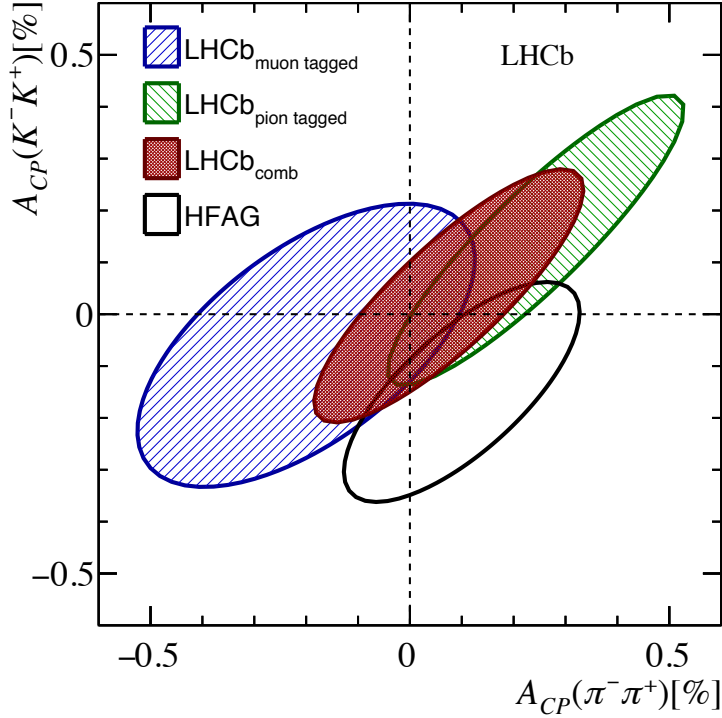
Figure 11: Current status of time-integrated CP violation in $D^0 \rightarrow K^+K^-$ and $D^0 \rightarrow \pi^+\pi^-$ decays. The dashed green ellipse is obtained using the present $D^0 \rightarrow K^+K^-$ result. The dashed blue ellipse shows previous results which used semileptonic B decays and a muon-tagged technique. The red filled ellipse represents the combination of both measurements. The black ellipse shows a world combination made by the Heavy Flavor Averaging Group, which includes the results of other experiments as well as older LHCb results.

Figure 11 summarises the current situation in the $A_{CP}(K^+K^-)$ versus $A_{CP}(\pi^+\pi^-)$ plane. As apparent, there is no evidence for CP violation yet. Furthermore, time-dependent CP asymmetries in the $D^0 \rightarrow K^+K^-$ and $D^0 \rightarrow \pi^+\pi^-$ decay rates were measured using the same data sample. The asymmetries in effective decay widths between D^0 and $\overline{D}^0$ decays, sensitive to indirect CP violation, were measured using two different experimental approaches [10, 11]. These measurements are consistent with CP conservation and improve by nearly a factor two the previous world-leading measurements, also obtained by LHCb using the 2011 subsample of the current data.

In the beauty sector, a time-dependent angular analysis of $B_s^0 \rightarrow \psi(2S)\phi$ decays was performed with the full Run 1 data [12]. The CP-violating phase and decay-width difference of the B_s^0 system were measured. This is the first time that ϕ_s and $\Delta\Gamma_s$ are measured in a decay containing the $\psi(2S)$ resonance. Another time-dependent analysis was performed in the decay channel $B^0 \rightarrow D^+D^-$ with

Run 1 data [13]. The *CP*-violating observables S and C were determined. The observable S describes *CP* violation in the interference between mixing and the decay amplitude, and C parametrises direct *CP* violation in the decay.

A very interesting result was obtained when searching for *CP*-violating asymmetries in the decay angle distributions of Λ_b^0 baryons decaying to $p\pi^-\pi^+\pi^-$ and $p\pi^-K^+K^-$ final states [14]. These four-body hadronic decays are a promising place to search for sources of *CP* violation both within and beyond the Standard Model. Evidence for *CP* violation in $\Lambda_b^0 \to p\pi^-\pi^+\pi^-$ decays was found with a statistical significance corresponding to 3.3 standard deviations. This represents the first evidence for *CP* violation in the baryon sector.

5   Financial issues

The status of the accounts is healthy and no cash flow problems are foreseen. The expenditure on the 2016 M&O Cat. A budget has followed forecasts. LHCb has recorded an underspending on the M&O Cat. A budget in 2015, due to a delayed recruitment of an online system manager and to late bills. Part of this surplus was already used to consolidate the farm. From the year 2016, LHCb proposed a 2% decrease in the M&O Cat. A budget, which was accepted. The number of PhD equivalent keeps on increasing and it now exceeds 500.

6   Collaboration matters

At the LHCb Collaboration Board (CB) meeting of September 2016 Tomsk Polytechnic University, Russia, was accepted as an associated institute of the collaboration. Valerie Gibson from the Cavendish Laboratory, University of Cambridge, was elected new CB chair, and will take over from current chair, Bernhard Spaan, from the Technical University of Dortmund, in December 2016.

References

[1] LHCb collaboration, *Central exclusive production of J/ψ and $\psi(2S)$ mesons in pp collisions at $\sqrt{s} = 13\,TeV$,* LHCb-CONF-2016-007.

[2] LHCb collaboration, R. Aaij *et al.*, *Measurement of the b production cross-section in 7 and 13 TeV pp collisions,* LHCb-PAPER-2016-031, in preparation.

[3] LHCb collaboration, R. Aaij *et al.*, *Measurement of the forward Z boson production cross-section in pp collisions at $\sqrt{s} = 13\,TeV$,* arXiv:1607.06495, submitted to JHEP.

[4] LHCb collaboration, R. Aaij *et al.*, *Observation of exotic $J/\psi\phi$ structures from amplitude analysis of $B^+ \to J/\psi\phi K^+$ decays,* arXiv:1606.07895, submitted to Phys. Rev. Lett.

[5] LHCb collaboration, R. Aaij *et al.*, *Amplitude analysis of $B^+ \to J/\psi\phi K^+$ decays,* arXiv:1606.07898, submitted to PRD.

[6] LHCb collaboration, *Evidence for the rare decay $\Sigma^+ \to p\mu^+\mu^-$,* LHCb-CONF-2016-013.

[7] LHCb collaboration, R. Aaij *et al.*, *Observation of the annihilation decay mode $B^0 \to K^+K^-$,* LHCb-PAPER-2016-036, in preparation.

[8] LHCb collaboration, R. Aaij *et al.*, *First measurement of the photon polarization in radiative B_s^0 decays,* LHCb-PAPER-2016-034, in preparation.

[9] LHCb collaboration, R. Aaij *et al.*, *Measurement of CP asymmetry in $D^0 \to K^+K^-$ decays,* LHCb-PAPER-2016-035, in preparation.

[10] LHCb collaboration, *Measurement of time-dependent CP-violating asymmetries in $D^0 \to K^+K^-$ and $D^0 \to \pi^+\pi^-$ decays,* LHCb-CONF-2016-009.

[11] LHCb collaboration, *Measurement of the CP violation parameter A_Γ with 2012 data,* LHCb-CONF-2016-010.

[12] LHCb collaboration, R. Aaij *et al.*, *Measurement of the CP violating phase and decay-width difference in $B_s^0 \to \psi(2S)\phi$ decays,* arXiv:1608.04855, submitted to Phys. Lett. B.

[13] LHCb collaboration, R. Aaij *et al.*, *Measurement of CP violation in $B \to D^+D^-$ decays,* arXiv:1608.06620, submitted to Phys. Rev. Lett.

[14] LHCb collaboration, R. Aaij *et al.*, *Probing matter-antimatter asymmetries in beauty baryon decays,* LHCb-PAPER-2016-030, in preparation.

[15] LHCb collaboration, *Status of the LHCb upgrade,* CERN-RRB-2016-111.

[16] LHCb collaboration, *Status of the LHCb experiment*, CERN-RRB-2016-31.

[17] C. Bozzi, *LHCb Computing Resource usage in January–July 2016*, Tech. Rep. LHCb-PUB-2016-023. CERN-LHCb-PUB-2016-023, CERN, Geneva, Aug, 2016.

[18] C. Bozzi, *LHCb Computing Resources: reassessment of 2017 requests and preview of 2018 and 2019 requests*, Tech. Rep. LHCb-PUB-2016-022. CERN-LHCb-PUB-2016-022, CERN, Geneva, Aug, 2016.